SELECTIVE LASER MELTING OF COPPER BASED ALLOY ON STEEL: A PRELIMINARY STUDY

CHER FU TEY
School of Mechanical and Aerospace Engineering, Nanyang Technological University, 50 Nanyang Avenue, Singapore 639798, Singapore

WAI YEE YEONG, SONGLIN CHEN
Singapore Centre for 3D Printing, SC3DP Future of Manufacturing Lab 1, 2A Nanyang Link, HW1-01-05, Singapore 637372, Singapore

ABSTRACT: The constantly increasing requirements of critical engineering parts can often be satisfied through the use of different materials with unique properties. In an effort to realize the potential of multi-functional parts, a study on the melt track characteristics of a copper based alloy (HOVADUR® K220) deposited on 316L steel via Selective Laser Melting (SLM) has been conducted. Single-line melt tracks, processed using 3 different sets of laser parameters, were printed on top of copper based alloy of variable height. It was found that the widths of the line tracks decreased with the height of the copper alloy. When processed at an energy density of 262J/mm3 the width of the copper alloy line tracks decreased from an average of 332μm to 151μm as the layers of underlying copper alloy increased from 0 to 40. Extensive cracking was observed when excessive energy density was used on layers 1 to 6. All scan tracks are continuous with minor amounts of unmelted particles. Track stability is observed to decrease slightly at higher layers as the track width decreases.

KEYWORDS: multi-material printing, selective laser melting, copper alloy, steel

INTRODUCTION

The multi-disciplinary nature of engineering applications today often has several functional and structural requirements to fulfill. Creating a component which has an optimal balance of properties may require different materials to be used in the same part. Within the metallic class of materials, there are many methods that can be used to create a bond between dissimilar alloys. Solid state bonding techniques such as diffusion bonding has been used to join metals either with or without the use of an intermediate bond layer (Kundu et al. 2005). Explosion bonding has been used to join dissimilar metals such as copper and steel for applications that require both structural integrity as well as thermal shielding properties (Leedy & Stubbins 2001). Laser welding has also been used to melt and fuse different metals (Chen et al. 2013). Lately, additive manufacturing has also displayed the capability to produce multi-material parts (Al-Jamal et al. 2008, Sing et al. 2015, Sahasrabudhe et al. 2015) as well as parts made from bimetallic powder blend (Sing et al. 2016, Sing et al. 2015). Unlike the other joining techniques, additively manufactured multi-materials part does not require the user to first have 2 solid parts prior to joining. Hence, the geometry of a join produced through AM is not restricted by the profile of the original solid parts and higher geometrical complexity can potentially be achieved. However, these potential advantages of additively manufactured multi-material parts may only be realized after the interfacial bond properties at are adequately characterized. The interface, which has high amount of material property mismatch, is usually the critical area of concern. By far most research work on the SLM of bimetallic systems have employed a single laser parameter to process the entire interface (Liu et al. 2014, Sahasrabudhe et al. 2015). Due to the intermixing of the 2 materials, the interface

Proc. of the 2nd Intl. Conf. on Progress in Additive Manufacturing
Edited by Chee Kai Chua, Wai Yee Yeong, Ming Jen Tan, Erjia Liu and Shu Beng Tor

Published by Research Publishing, Singapore
ISSN: 2424-8967

inherently has a material composition gradation that changes from 100% of material 'A' to 100% of material 'B'. To maintain similar melt track morphology across the interface despite the composition gradation would require a range of laser processing parameters. On the other hand, if only a single set of laser parameter was used, the melt track morphology is then expected to vary continuously within the interface. In this study, line tracks were deposited on the top surface of a copper alloy (HOVADUR® K220) printed on bases made from 316L stainless steel (Figure 1b). The laser parameter and height of the copper alloy were varied to investigate its effects on the line track characteristics. The width, appearance and stability of the line tracks are examined under optical microscope to evaluate the suitability of the different laser parameters.

EXPERIMENTAL SETUP

The machine used for this experiment is the SLM250HL. It is equipped with a Gaussian beam fiber laser having a focal diameter of 80μm. 10 mm line tracks, processed using 3 different sets of laser parameters, were printed on top of a variable thickness copper alloy which is printed over a 316L steel base (Figure 1a &1b). The line tracks were printed on the 1st, 6th, 11th, 21st, 31st and 41st layers. When the line tracks are printed on the 1st layer, it is implied that they are printed directly over the 316L steel base without any copper alloy layers in between. Similarly, line tracks printed on the 31st layer would have 30 underlying layers of copper alloy. The laser parameters used in the 3 different configurations are shown in Table 1. Melt track stability and width measurements were performed on an optical microscope.

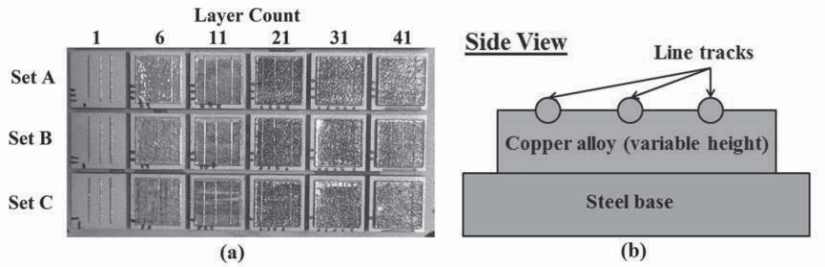

Figure 1. (a) Top view of printed samples, (b) Illustration of the front view of specimen

Table 1: Laser parameters

	Set A (High energy)	Set B (Moderate energy)	Set C (Low energy)
Laser Power, P (W)	375	375	375
Scanning Speed, V (mm/s)	300	530	800
Hatch Spacing, h (μm)	90	90	90
Layer Thickness, t (μm)	30	30	30
Energy Density, E (J/mm^3)	463	262	174

RESULTS AND DISCUSSIONS

Effects of copper alloy thickness on line track width

Five width measurements were randomly taken along each line track on the same sample and the average widths are plotted in Figure 2. Regardless of the laser parameter all track widths are observed to decrease as the layers/height of copper alloy increases. This change in width can also

be observed from the optical images of the scan tracks in Figure 3. The decrease in width can be explained through the thermal conductivities of both materials. According to the data from SCHMELZMETALL, HOVADUR® K220 has an average thermal conductivity of 220W/m/K between temperatures of 293 to 573K. Compared to the 13-34W/m/K for 316L stainless steel at temperatures between 300 to 1500K (Kim 1975), the conductivities of both alloys are drastically different. In the first layer when the copper alloy is printed directly on 100% 316L stainless steel, a high amount of heat energy is being retained in the melt pool due to low conduction loss through the underlying low conductivity steel material. This causes the melt pool to be significantly larger, leading to wider width measurements. As more layers of copper alloy were printed over the 316L stainless steel base, the top surface of the sample would experience a composition shift from 100% 316L stainless steel towards 100% copper alloy. This shift causes the average thermal conductivity of the top layer to increase and subsequently lead to higher conduction loss and narrower melt pool on the next printed layer. Eventually, when the composition of the top layer approaches that of the copper alloy, the track width stabilizes and levels off to fixed values as shown in Figure 2. Naturally, the stabilized track widths are different for the 3 laser settings. The narrowest stabilized width corresponds to the highest scanning velocity (lowest energy density) and vice versa. To keep the porosities within a part to a minimum, adjacent tracks must have a certain amount of overlap. Intuitively, when the hatch spacing is too large, insufficient overlap introduces gaps and porosity between tracks. However, overly narrow hatch spacing may also lead to increased porosity (Yadroitsev et al. 2007, Thijs et al. 2010). Although the reason of increased porosity due to excessive overlap is not well understood, it will be assumed that there exists an optimal hatch spacing and track overlap that will give maximum part density. If indeed a fixed amount of overlap is necessary for optimal density, there is a need to constantly vary the hatch distance in the intermix region to match the decreasing track width across the interface. If a 40% overlap between tracks is desired, one may set the hatch spacing to take a value that is 40% of the width measurements at different layers, assuming that the track width is independent of hatch spacing. Even though the underlying assumption is flawed and may lead to slight errors in the resultant track overlaps, the proposed method serves as a starting point to achieve the desired overlap. The smallest width of the melt track processed at 800mm/s is 118±19μm. Even if fluctuations are taken into account, this value is still slightly larger than the 90 μm hatch spacing. Hence there is still overlap between adjacent tracks.

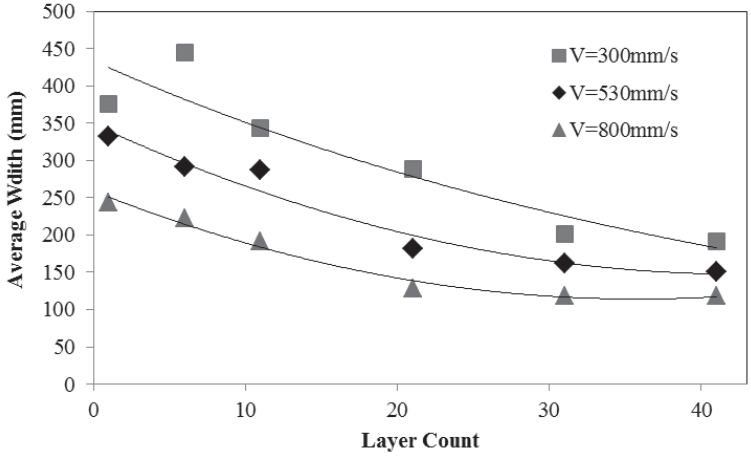

Figure 2. Track width vs. layer count (power: 375W, layer thickness: 30μm, hatch: 90μm)

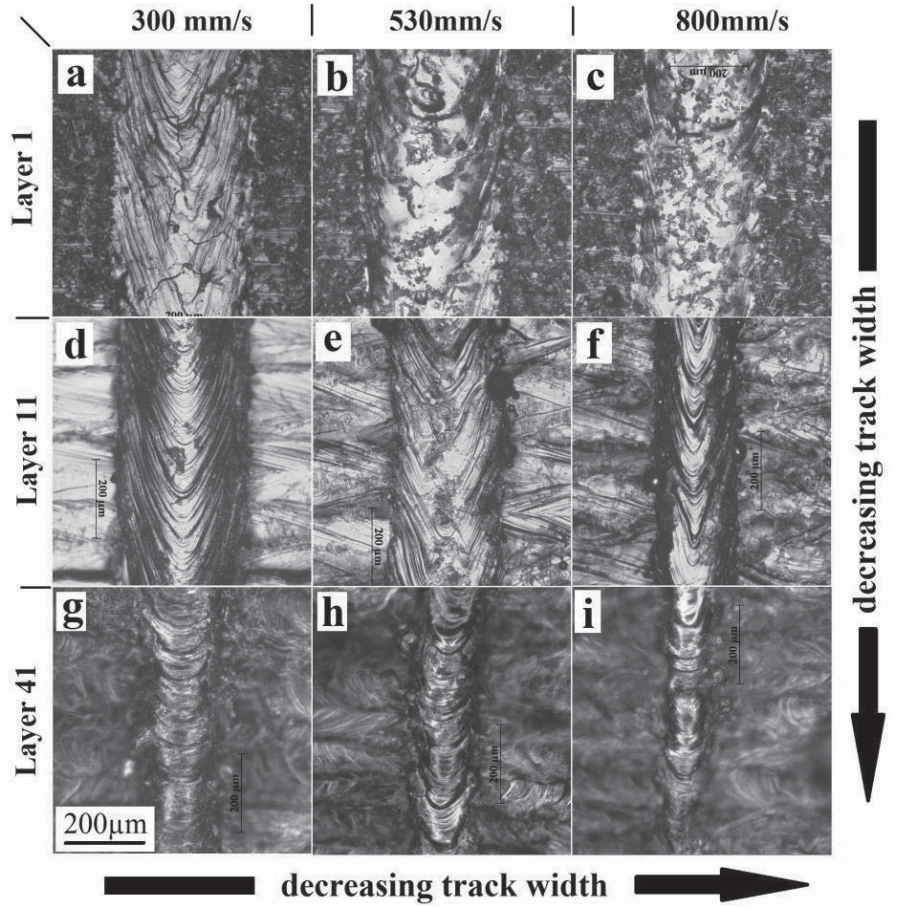

Figure 3. Appearance of the melt tracks procesed at different heights and laser velocity (P=375W)

Continuity and stability of melt tracks

The continuous appearance of all the tracks with minor amounts of unmelted particles attached indicates good melt pool stability. However, as the tracks get thinner with layer count and scanning speed, the perturbations due to surface roughness becomes large relative to the dimensions of the scan tracks. Furthermore, at high scanning speeds, the melt pool becomes longer and narrower. If we assume that the melt pool can be approximated as a circular cylinder of molten liquid attached to the solid base through a single line of contact, then according to Yadroitsev et al. the necessary and sufficient condition for stability is:

$$\frac{\pi D}{L} > \sqrt{\frac{2}{3}} \qquad (1)$$

where L is the wavelength that corresponds to the perturbations and D is the diameter of the cylinder (Yadroitsev et al. 2010). Clearly when the width and hence the circumference of the melt pool decreases, the above condition for stability becomes harder to satisfy. From Figure 4i, irregularities in the tracks have resulted in a significantly different track width measurement at the top and bottom of the picture. Even though balling has not occurred, it is believed to be imminent following further increase in scanning speed.

Surface cracks on melt tracks

As shown in Figure 3a, obvious cracks can be observed on the tracks printed in the first layer using the high energy density parameter. These cracks were also visible on the surface of the 6th layer (Figure 4) but disappeared on the 11th layer (Figure 3d). The same laser setting that induced excessive residual stress and caused crack initiation and propagation from layers 1 to 6 appeared to be suitable for layers 11 and beyond. This again suggests the need to adopt different laser parameters across the intermix region. The cracks that appear in the SLM of a single material are likely caused by large differential cooling which induced excessive residual stresses and mismatch strains. However, in the SLM of bimetallic systems the dilution of the deposited layer becomes an added consideration, i.e. the extent of mixing between the scan track and the underlying layers (Hofman et al. 2011). When dissimilar metals are fused together, their different thermophysical properties create even greater mismatch strains during solidification and cooling. Furthermore, the mixing of 2 alloys may also produce brittle phases that could further aggravate the situation. The cracks in this bimetallic print on layers 1 to 6 were certainly caused by the coupled effects of cooling, material and phase composition. It may not be justifiable to consider these effects in isolation to determine the cause of cracking. What will be said for now is that the unique combination of these factors for each laser parameter is responsible for crack initiation and propagation. As to whether there is a more predominant factor is a topic for future research.

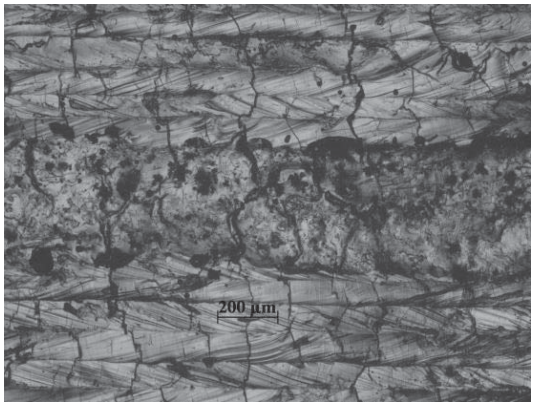

Figure 4. Extensive cracking on layer 6, V=300mm/s

CONCLUSION

Line tracks were deposited on the top surface of copper alloys samples that were printed on stainless steel bases. The height of the copper alloy and the laser setting were varied to investigate their effects on the melt track morphology. The findings are:

- Width of melt track decreases with the height of copper alloy for each laser setting due to increased conduction loses.
- Line tracks were continuous with minor amount of unmelted particles for all combinations of laser settings and copper thickness investigated in this study. Stability was observed to deteriorate slightly as the track width became narrower at higher scanning speed and build heights.
- The high energy density laser parameter that produced tracks with extensive surface cracks from layers 1 to 6 is capable of producing crack-free tracks from layer 11 onwards. This emphasizes the need for a range of laser parameter across the interface between 2 materials.

ACKNOWLEDGMENTS

The authors wish to acknowledge the National Research Foundation for the funding as well as Singapore Centre for 3D Printing and Nanyang Technological University School of Mechanical and Aerospace Engineering for their laboratory facilities.

REFERENCES

Kundu, S., Ghosh, M., Laik, A., Bhanumurthy, K., Kale, G.B. and Chatterjee, S., 2005. Diffusion bonding of commercially pure titanium to 304 stainless steel using copper interlayer. Materials Science and Engineering: A, 407(1), pp.154-160.

Leedy, K.D. and Stubbins, J.F., 2001. Copper alloy–stainless steel bonded laminates for fusion reactor applications: crack growth and fatigue. Materials Science and Engineering: A, 297(1), pp.19-25.

Chen, S., Huang, J., Xia, J., Zhang, H. and Zhao, X., 2013. Microstructural characteristics of a stainless steel/copper dissimilar joint made by laser welding. Metallurgical and Materials Transactions A, 44(8), pp.3690-3696.

Al-Jamal, O.M., Hinduja, S. and Li, L., 2008. Characteristics of the bond in Cu–H13 tool steel parts fabricated using SLM. CIRP Annals-Manufacturing Technology, 57(1), pp.239-242.

Sing, S.L., Lam, L.P., Zhang, D.Q., Liu, Z.H. and Chua, C.K., 2015. Interfacial characterization of SLM parts in multi-material processing: Intermetallic phase formation between AlSi10Mg and C18400 copper alloy. Materials Characterization, 107, pp.220-227.

Sahasrabudhe, H., Harrison, R., Carpenter, C. and Bandyopadhyay, A., 2015. Stainless steel to titanium bimetallic structure using LENS™. Additive Manufacturing, 5, pp.1-8.

Sing, S.L., Yeong, W.Y. and Wiria, F.E., 2016. Selective laser melting of titanium alloy with 50 wt% tantalum: Microstructure and mechanical properties. Journal of Alloys and Compounds, 660, pp.461-470.

Sing, S.L., An, J., Yeong, W.Y. and Wiria, F.E., 2015. Laser and electron-beam powder-bed additive manufacturing of metallic implants: A review on processes, materials and designs. Journal of Orthopaedic Research, 34, pp.369-385.

Liu, Z.H., Zhang, D.Q., Sing, S.L., Chua, C.K. and Loh, L.E., 2014. Interfacial characterization of SLM parts in multi-material processing: Metallurgical diffusion between 316L stainless steel and C18400 copper alloy. Materials Characterization, 94, pp.116-125.

Kim, C.S., 1975. Thermophysical properties of stainless steels (No. ANL--75-55). Argonne National Lab., Ill.(USA). doi:10.2172/4152287. http://www.osti.gov/scitech/servlets/purl/4152287.

Yadroitsev, I., Thivillon, L., Bertrand, P. and Smurov, I., 2007. Strategy of manufacturing components with designed internal structure by selective laser melting of metallic powder. Applied Surface Science, 254(4), pp.980-983.

Thijs, L., Verhaeghe, F., Craeghs, T., Van Humbeeck, J. and Kruth, J.P., 2010. A study of the microstructural evolution during selective laser melting of Ti–6Al–4V. Acta Materialia, 58(9), pp.3303-3312.

Yadroitsev, I., Gusarov, A., Yadroitsava, I. and Smurov, I., 2010. Single track formation in selective laser melting of metal powders. Journal of Materials Processing Technology, 210(12), pp.1624-1631.

Hofman, J.T., De Lange, D.F., Pathiraj, B. and Meijer, J., 2011. FEM modeling and experimental verification for dilution control in laser cladding. Journal of Materials Processing Technology, 211(2), pp.187-196.